

ON THE STELLAR MASSES OF GIANT CLUMPS IN DISTANT STAR-FORMING GALAXIES

MIROSLAVA DESSAUGES-ZAVADSKY,¹ DANIEL SCHAEERER,^{1,2} ANTONIO CAVA,¹ LUCIO MAYER,^{3,4} AND
VALENTINA TAMBURELLO^{3,4}

¹*Observatoire de Genève, Université de Genève, 51 Ch. des Maillettes, 1290 Versoix, Switzerland*

²*CNRS, IRAP, 14 Avenue E. Belin, 31400 Toulouse, France*

³*Center for Theoretical Astrophysics and Cosmology, Institute for Computational Science, University of Zurich, Winterthurerstrasse 190, 8057 Zürich, Switzerland*

⁴*Physik-Institut, University of Zurich, Winterthurerstrasse 190, 8057 Zürich, Switzerland*

(Received; Revised; Accepted)

Submitted to ApJL

ABSTRACT

We analyse stellar masses of clumps drawn from a compilation of star-forming galaxies at $1.1 < z < 3.6$. Comparing clumps selected in different ways, and in lensed or blank field galaxies, we examine the effects of spatial resolution and sensitivity on the inferred stellar masses. Large differences are found, with median stellar masses ranging from $\sim 10^9 M_{\odot}$ for clumps in the often-referenced field galaxies to $\sim 10^7 M_{\odot}$ for fainter clumps selected in deep-field or lensed galaxies. We argue that the clump masses, observed in non-lensed galaxies with a limited spatial resolution of ~ 1 kpc, are artificially increased due to the clustering of clumps of smaller mass. Furthermore, we show that the sensitivity threshold used for the clump selection affects the inferred masses even more strongly than resolution, biasing clumps at the low mass end. Both improved spatial resolution and sensitivity appear to shift the clump stellar mass distribution to lower masses, qualitatively in agreement with clump masses found in recent high-resolution simulations of disk fragmentation. We discuss the nature of the most massive clumps, and we conclude that it is currently not possible to properly establish a meaningful clump stellar mass distribution from observations and to infer the existence and value of a characteristic clump mass scale.

Keywords: galaxies: evolution — galaxies: high-redshift — galaxies: structure

arXiv:1702.00055v1 [astro-ph.GA] 31 Jan 2017

1. INTRODUCTION

Deep *Hubble Space Telescope* (*HST*) observations and pioneering morphological analysis of distant star-forming galaxies have revealed that galaxies at the peak of the cosmic star formation activity do not follow the *Hubble* classification, but are mostly irregular and clumpy (Elmegreen et al. 2005, 2007, 2009). Guo et al. (2015) and Shibuya et al. (2016) have evaluated that at $z \gtrsim 2$ roughly 60% of galaxies are clumpy and that this fraction evolves over $z \simeq 0 - 8$.

While the observed stellar clumps have initially been associated with interactions/mergers, another clump origin had to be invoked with kinematic studies showing a substantial proportion of $z \sim 1 - 2.5$ galaxies dominated by ordered disk rotation (Förster Schreiber et al. 2009; Wisnioski et al. 2015; Rodrigues et al. 2016). These high-redshift disks, however, are very different from their local counterparts, being highly turbulent, thick, gas-rich, and strongly star-forming disks. They are subject to violent instabilities (Dekel et al. 2009b) caused by intense inflows of cold gas (Kereš et al. 2005; Ocvirk et al. 2008; Dekel et al. 2009a). Giant kpc-scale clumps with masses as high as $\gtrsim 10^8 - 10^{9.5} M_\odot$ may then form during the disk fragmentation phase resulting from disk instabilities, as found in idealized simulations of isolated galaxies and cosmological simulations (Agertz et al. 2009; Bournaud et al. 2010, 2014; Ceverino et al. 2010, 2012; Genel et al. 2012; Mandelker et al. 2014). The produced giant clumps resemble the kpc-sized clumps observed in $z \sim 2$ galaxies with similar stellar masses (Förster Schreiber et al. 2011; Guo et al. 2012), and provide support to clump formation via disk fragmentation.

Recently, Tamburello et al. (2015, hereafter T15) and Behrendt et al. (2016) performed numerical simulations of isolated galaxies at a significantly better spatial resolution, necessary to capture fragmentation correctly (Mayer & Gawryszczak 2008). They both find that the formation of giant clumps via disk fragmentation with masses $> 10^8 M_\odot$ is *not* a common occurrence. They get the same characteristic clump mass set by fragmentation, as low as a few times $10^7 M_\odot$, despite significant differences in their respective simulation techniques, and star formation and feedback recipes only included in T15. This fragmentation mass is well matched with the modified Toomre mass proposed by T15 that takes into account nonlinear aspects of disk fragmentation (Boley et al. 2010). A few clumps can grow to larger masses ($\sim 10^{9-9.5} M_\odot$) by clump-clump mergers and gas accretion, but they populate only the tail of the mass distribution and emerge after several disk orbits. The conventional Toomre mass, resulting from simple linear

perturbation theory (Toomre 1964), is almost an order of magnitude larger, and hence appears only fortuitously comparable to the clump high mass tail. A similar mass spectrum ranging from $\sim 10^{6.5} M_\odot$ to $10^{9.5} M_\odot$ is obtained for the ‘in situ’ clumps formed in the recent high-resolution cosmological simulations by Mandelker et al. (2017), as well as in the FIRE cosmological simulations by Oklopčić et al. (2017).

Now that disk fragmentation simulations of different groups find significantly lower masses for the high-redshift clumps with respect to previous claims, it is timely to revisit the observational constraints on clump masses. In this Letter, we compile a sample of clumps in star-forming galaxies at $1.1 < z < 3.6$ with stellar mass measurements. We show that a very broad range of clump masses has been derived, and find evidence that the derived masses and mass distributions suffer from limitations in both spatial resolution and sensitivity. We discuss what we may infer on the true stellar mass spectrum of high-redshift clumps. Our simple qualitative analysis presented here highlights important biases affecting the intrinsic clump stellar mass estimates, which we have started quantitatively evaluating in our first companion paper on $H\alpha$ mock simulations (Tamburello et al. 2016, hereafter T16) and in a detailed observational clump analysis within a multiple-imaged galaxy (Cava et al. in preparation).

2. CLUMP SAMPLE

We have compiled a sample of clumps from the literature within clumpy star-forming galaxies at $z > 1$, where clumps have been identified in broad-band *HST* imaging, predominantly tracing stellar emission. Our sample comprises a total of 241 stellar clumps hosted in 40 galaxies from Förster Schreiber et al. (2011), Guo et al. (2012), Adamo et al. (2013), Elmegreen et al. (2013), and Wuyts et al. (2014). These five clump datasets are described in Table 1. For the bulk of the sample (213 out of 241 clumps), we have been able to recompute the clump stellar masses in a homogeneous way, using the original multi-band *HST* photometry and the updated version of the *Hyperz* photometric redshift and SED fitting code (Schaerer & de Barros 2010). For the remaining 28 clumps from Förster Schreiber et al. (2011), as observations in only one *HST*/NICMOS filter F160W are available, we have not re-analysed their published stellar masses, instead we rely on these estimates obtained from an assumed mass-to-light ratio.

The photometry of the stellar clumps from Guo et al. (2012) and Elmegreen et al. (2013) is based on the *Hubble* Ultra Deep Field observations (HUDF, Beckwith et al. 2006), performed with *HST*/ACS in the fil-

ters F435W, F606W, F775W, and F850LP. Guo et al. (2012) also used the *HST*/WFC3 observations in the filters F105W, F125W, and F160W, which were not available at the time of the Elmegreen et al. (2013) work. Adamo et al. (2013) have used the Cluster Lensing And Supernova survey with *Hubble* (CLASH, Postman et al. 2012) to analyse clumps in the filters F390W, F475W, F555W, F606W, F775W, F814W, and F850LP from *HST*/ACS, and the filters F105W, F110W, F125W, and F160W from *HST*/WFC3. And, Wuyts et al. (2014) had at disposal observations in the *HST*/WFC3 filters F390W, F606W, F814W, F098M, F125W, and F160W. For the typical redshift $z \sim 2$ of the studied clumpy host galaxies, the longest wavelength observations available at $1.6 \mu\text{m}$ for all cover the rest-frame optical emission of the stellar clumps.

For the SED modelling, we have adopted the Bruzual & Charlot (2003) stellar tracks at solar metallicity and the Chabrier (2003) initial mass function. We have allowed for variable star formation histories, parametrised by exponentially declining models with timescales varying from 10 Myr to infinity¹, corresponding to a constant star formation rate. Nebular emission has been neglected, as in Guo et al. (2012) and Elmegreen et al. (2013). With respect to these works, we find very small or no systematic differences with our inferred clump stellar masses². We have also tested the impact on clump stellar masses when including or not the near-infrared *HST*/WFC3 photometry in the dataset of Guo et al. (2012). We find higher stellar masses by +0.20 dex, on average, when the *HST*/WFC3 filters are omitted, as done in Elmegreen et al. (2013). This could thus lead to a small systematic shift by a factor of ~ 1.5 between the clump masses of Guo et al. (2012) and Elmegreen et al. (2013). Compared to the clump stellar masses reported by Adamo et al. (2013), our masses are higher by +0.56 dex, on average. This difference vanishes³ if we include nebular emission and allow for ages younger than 10 Myr in the SED fits, as adopted by Adamo et al. (2013). For the Wuyts et al. (2014) dataset, we find a small difference of -0.12 dex, on average, in clump stellar masses when neglecting nebular emission, as in their work. For a uniform and conservative comparison between all the clump datasets, we retain the clump

stellar masses obtained from SED fits *without* nebular emission.

The wavelength coverage of the above four clump datasets is nearly identical, which thus enables a meaningful and nearly homogeneous comparison between these datasets. As a measure of the depth of the selected clumps, we examine the clump magnitude distributions and we list in Table 1, for the four clump datasets, the magnitudes i_{16} and z_{16} corresponding to the 16th percentile of the magnitude distribution of clumps in the F775W (for HUDF) or F814W i -band and in the F850LP z -band, respectively. The latter corresponds to the clump selection band of Guo et al. (2012), and the former is the second-deepest band in HUDF and CLASH. We also indicate the 3σ sensitivity limits in the i - and z -bands measured in $0.35''$ diameter apertures, as reported by Beckwith et al. (2006) for HUDF and Postman et al. (2012) for CLASH. On this basis, we divide the clumpy host galaxy compilation into three main sub-samples, lensed galaxies, field galaxies with a deep clump selection, and field galaxies with a shallow clump selection, denoted hereafter by L, FD, and FS, respectively (see Table 1).

The 40 host galaxies have redshifts ranging from $z = 1.1$ to 3.6, with the bulk found at $1.3 < z < 2.6$. Their stellar masses are uniformly distributed between $M_*^{\text{host}} \sim 10^8 - 10^{11} M_\odot$ (see Figure 3), with the L and FD sub-samples containing the low-mass host galaxies ($M_*^{\text{host}} \lesssim 10^{10} M_\odot$) and the FS sub-sample the high-mass hosts ($M_*^{\text{host}} \gtrsim 10^{9.8} M_\odot$). Most of the hosts are on the main sequence at their corresponding redshift.

For comparison we also consider local star clusters found in nearby galaxies (Adamo et al. 2013) and two starburst galaxies (Bastian et al. 2006; Larsen et al. 2002).

3. CAN WE INFER ACCURATE CLUMP MASSES AT HIGH REDSHIFT?

As shown in Figure 1, the distribution of stellar masses of clumps identified in high-redshift galaxies is very broad and ranges from $M_*^{\text{clump}} \sim 10^{5.5} M_\odot$ to $10^{10.5} M_\odot$. Large differences are observed among the three sub-samples of high-redshift galaxies considered here. Whereas the “typical” mass of clump masses in the field galaxies studied by Förster Schreiber et al. (2011) and Guo et al. (2012) (FS sub-sample) – used until now as the benchmark of high-redshift clump properties – is very high (median $\log(M_*^{\text{clump,FS}}/M_\odot) = 8.89$), the Elmegreen et al. (2013) field galaxies (FD sub-sample) have a median clump mass much lower ($\log(M_*^{\text{clump,FD}}/M_\odot) = 7.23$), and clumps in lensed galaxies (L sub-sample) show even somewhat lower

¹ More precisely, we have used the following timescales $\tau = 0.01, 0.03, 0.05, 0.07, 0.1, 0.3, 0.5, 0.7, 1., 3., \infty$ Gyr.

² The mean of the logarithmic differences in stellar mass is $\Delta(\log(M_*^{\text{clump}}/M_\odot)) = -0.16 \pm 0.15$ for clumps from Guo et al. (2012), and $\Delta(\log(M_*^{\text{clump}}/M_\odot)) = +0.045 \pm 0.45$ for clumps from Elmegreen et al. (2013).

³ $\Delta(\log(M_*^{\text{clump}}/M_\odot)) = +0.004 \pm 0.46$.

Table 1. Properties of existing stellar clump datasets in high-redshift galaxies

References	Adamo+13	Wuyts+14	Elmegreen+13	Guo+12	Förster Schreiber+11
	L sub-sample ^a		FD sub-sample ^b		FS sub-sample ^c
Number of clumps	31	7	135	40	28
Number of host galaxies	1	1	22	10	6
Redshift	1.5	1.7	1.1 – 3.6	1.6 – 2.0	2.2 – 2.5
i_{16} ^d	29.7 [†]	29.1 [‡]	29.7	27.6	–
i -band 3σ -0.35'' limit ^e	30.5 [†]	30.9 [‡]	30.25	30.25	–
z_{16} ^d	29.7 [†]	–	29.7	27.3	–
z -band 3σ -0.35'' limit ^e	29.5 [†]	–	29.55	29.55	–
Median $\log(M_*^{\text{clump}}/M_\odot)$	6.98		7.23		8.89

^aClumps identified in lensed galaxies.

^bClumps identified in field galaxies with a deep clump selection.

^cClumps identified in field galaxies with a shallow clump selection.

^dMagnitudes corresponding to the 16th percentile of the magnitude distribution of clumps in the F775W (for HUDF) or F814W i -band and in the F850LP z -band, respectively.

^e 3σ sensitivity limits in the i -, respectively, z -band measured in 0.35'' diameter apertures (from Beckwith et al. (2006) for HUDF and Postman et al. (2012) for CLASH).

[†]Corrected for lensing, assuming a magnification factor $\mu = 8$ (Adamo et al. 2013).

[‡]Corrected for lensing, assuming a magnification factor $\mu = 25$ (Sharon et al. 2012).

masses (median $\log(M_*^{\text{clump,FS}}/M_\odot) = 6.98$; see Table 1). In comparison to the star clusters identified in local galaxies, the inferred clump masses in high-redshift galaxies are, on average, significantly higher than those in local galaxies also shown in Figure 1, with the exception of some star clusters in the most intensively star-forming nearby galaxies.

The absolute rest-frame V -band magnitude distributions of the three clump sub-samples are compared in Figure 2. Clearly, the FS sub-sample has significantly brighter clumps than the FD sub-sample, although both are drawn from field galaxies over a similar redshift range. The clumps in the lensed galaxies are slightly fainter, on average, than those in the FD sub-sample. The differences in absolute magnitude and in stellar mass (Figure 2 versus Figure 1) are comparable, as expected, since the optical light traces stellar mass if the mass-to-light ratio of clumps does not vary much.

What explains the large differences found between the three sub-samples of high-redshift clumps? We primarily envisage *spatial resolution* and *sensitivity* as the main sources for these differences.

All high-redshift clumps rely on *HST* imaging with the same spatial resolution of $\sim 0.15''$ FWHM, which corre-

sponds to physical sizes of 1.2–1.3 kpc at $z \sim 1.3$ –2.6 in field/non-lensed galaxies. Obviously, limited spatial resolution can affect the measure of clump stellar masses, if the true physical sizes of clumps are smaller than the resolution, since then several clumps may be blended within the photometric aperture. This effect will artificially “boost” the flux and increase the inferred stellar mass of clumps. The amount of this artificial boost will depend on the clump true sizes, their distribution and clustering. With the help of strong gravitational lensing, sub-kpc sizes down to ~ 100 pc (representing an improvement by a factor of 10) are reached in the two lensed galaxies of the L sub-sample. The finding of considerably lower clump stellar masses (Figure 1 and Table 1) compared to the clump masses in the field galaxy sub-sample(s) (FS and somewhat FD) supports that indeed spatial resolution, and the induced blending, affects the derived clump masses and artificially boosts them towards high masses.

First quantitative hints of this low-resolution “boosting” on clump stellar masses have been obtained from recent simulations, which, however, focus on gas clumps. Behrendt et al. (2016), in their simulations of a massive gas disk with one of the highest resolutions to date, find

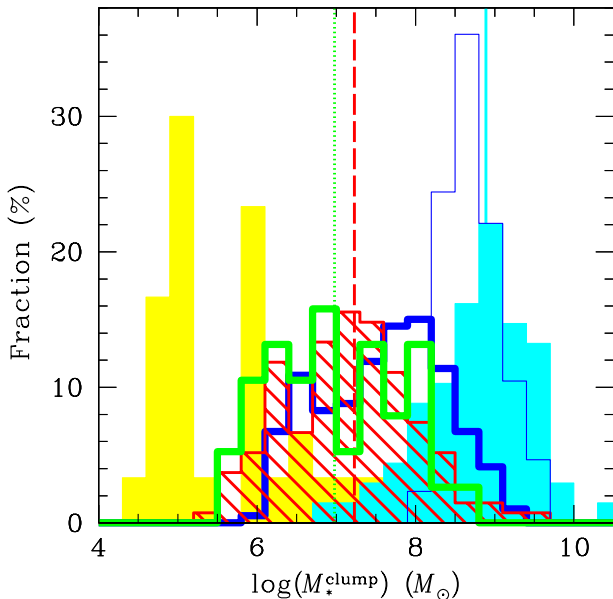


Figure 1. Normalized stellar mass distributions of local star clusters (filled yellow histogram), and three sub-samples of high-redshift clumps: clumps in lensed galaxies (L sub-sample, open green histogram), in field galaxies with a deep clump selection (FD sub-sample, hatched red histogram), and in field galaxies with a shallow clump selection (FS sub-sample, filled cyan histogram). The medians of the high-redshift clump sub-samples are shown using dotted green, dashed red, and solid cyan vertical lines, respectively. For comparison, clump mass distributions as predicted by different disk fragmentation simulations (open blue thick and thin histograms from T15 and Ceverino et al. (2012), respectively) are also shown in each panel.

very small (~ 35 pc in radii) and low gas mass fragments produced with disk fragmentation that, when mimicking observations on kpc-scales (FWHM = 1.6 kpc), appear to be distributed in loosely bound clusters with 10 – 100 times larger masses. We report similar results in T16 using our $H\alpha$ mock observations of simulations from T15, and we infer a ~ 1 kpc resolution “boosting” on 100 pc-scale clump masses of less than a factor of 5. Apart from that, Fisher et al. (2017), using low-redshift $H\alpha$ galaxy observations, have analysed how severely clump clustering increases sizes and star formation rates in limited ~ 1 kpc resolution maps.

Interestingly, large stellar mass differences are also observed between clumps in the field galaxy FS and FD sub-samples (Figure 1 and Table 1), while these galaxies are all affected by the same ~ 1.2 kpc resolution limitation. Another effect than spatial resolution must thus be at the origin of these clump mass differences. These differences are likely due to different clump selections applied, resulting from different data depths, different

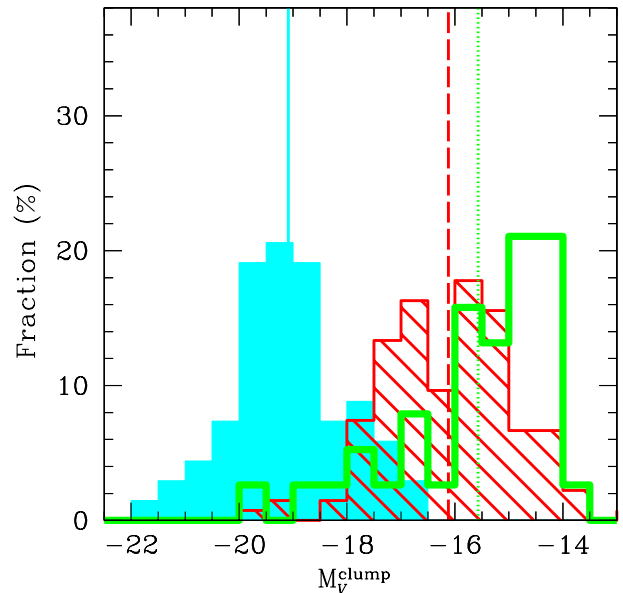


Figure 2. Absolute rest-frame V -band magnitude distributions of high-redshift clumps in the L (open green histogram), FD (hatched red histogram), and FS (filled cyan histogram) sub-samples. The respective means are shown using dotted green, dashed red, and solid cyan vertical lines.

wavebands used to identify the clumps, and/or more or less conservative detection limits set for clumps. In fact both Guo et al. (2012)⁴ and Elmegreen et al. (2013) used HUDF observations, but the former selected clumps in the F850LP z -band, whereas the latter in the F775W i -band that is 0.7 mag deeper (see Table 1). Furthermore, the clumps extracted by Guo et al. (2012) are limited to F850LP magnitudes brighter than ~ 27.3 , well above the depth of the HUDF z -band image. In contrast, the observed magnitudes of clumps selected by Elmegreen et al. (2013) reach down to 3σ , which can explain differences of up to ~ 2.5 mag for the faintest clumps in the FD sub-sample (see Table 1) compared to Guo et al. (2012). Hence, the clump selection sensitivity threshold strongly affects the clump stellar masses, biasing the observed clumps at the low mass end.

The sensitivity effect appears to be more important than the spatial resolution effect on the inferred clump masses, since the respective stellar mass distributions of clumps in the Elmegreen et al. (2013) field galaxies limited by ~ 1.2 kpc resolution (FD sub-sample) and in the lensed galaxies (L sub-sample) end up to be very comparable (Figure 1 and Table 1), whereas clumps in

⁴ The clumps from Guo et al. (2012) represent 60% of the clumps in the field galaxy FS sub-sample.

the lensed galaxies benefit from 10 times better spatial resolution *and* similarly good sensitivities.

In any case, the finding of clumps in lensed galaxies and in field galaxies from Elmegreen et al. (2013) with stellar masses between $\sim 10^{5.5} - 10^9 M_\odot$, well below the often-quoted “typical” masses of giant clumps $\gtrsim 10^8 - 10^9 M_\odot$ inferred from observations with ~ 1.2 kpc resolution and shallower clump selection thresholds (FS sub-sample), suggests that the latter is systematically overestimated by 1–2 orders of magnitude (Table 1), or more depending on whether a characteristic mass scale of fragmentation exists or not (see Section 4.2). The same conclusion can be drawn, when we restrict the FD and FS sub-samples to host galaxies with redshifts comparable to those of the two lensed galaxies from the L sub-sample. In T16 we study quantitatively the effects of ~ 1 kpc resolution and shallow sensitivity on the observed clump masses using H α mocks. We find that the inferred clump stellar masses can be easily overestimated by at least a factor of 10 due to the combination of both effects (and with the sensitivity effect dominating).

4. DISCUSSION

4.1. On the existence of the most massive clumps

Is there a maximum stellar mass for clumps, how massive, and what determines it? If clump stellar masses are artificially increased by the spatial resolution effect as discussed above, our current best maximum clump mass estimate should come from lensed galaxies, where clump stellar masses up to $\sim 10^{8.7} M_\odot$ are observed (see Figure 1). However, the L sub-sample is quite small (38 clumps) and small number statistics could bias the maximum mass determination of clumps (especially if the true clump mass function decreases rapidly towards high masses). Furthermore, the maximum clump stellar mass could depend on the host galaxy stellar mass (see Elmegreen et al. 2013). The fact that clumps in the FS and FD sub-samples, observed with the same spatial resolution in host galaxies spanning a wide range of stellar masses, show an increase of the upper envelope of their stellar masses with the host galaxy mass as illustrated in Figure 3, indicates that the maximum clump mass indeed depends on the host mass.

By definition, the clump mass cannot exceed the host galaxy mass, but what determines the maximum clump mass? The most simple expectation is that the maximum clump mass is set by the fragmentation mass that is directly proportional to the galaxy mass and the square of its gas fraction in the linear perturbation theory, as described by Escala & Larson (2008). Otherwise, according to the innovative simulations of T15, the combination of a typical fragmentation scale and addi-

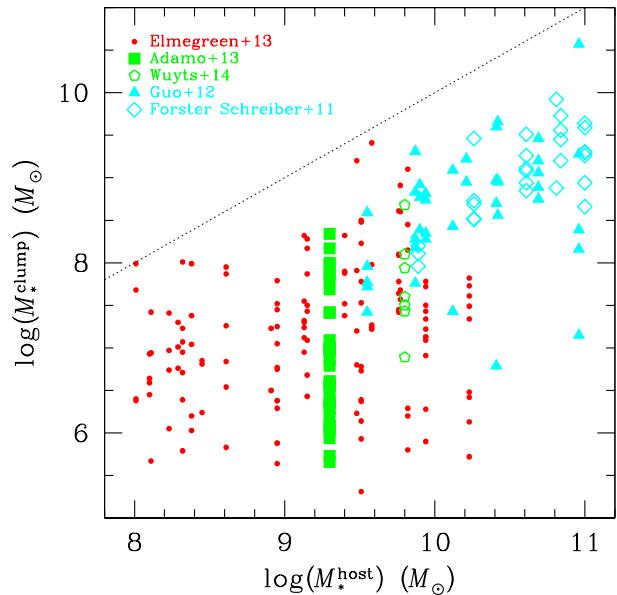


Figure 3. Stellar masses of high-redshift clumps plotted as a function of the stellar mass of their host galaxy. The symbols refer to different works, and the color-coding to the L, FD, and FS sub-samples, similarly to Figures 1 and 2. The dotted line is the one-to-one relation.

tional processes yielding the clump mass growth, such as clump-clump mergers, leads to a fractional stellar mass contribution of the sum of all clumps to the total disk stellar mass in the range of 10 – 15%, with little variation with disk mass. This results from the fact that the characteristic mass scale of fragmentation they get is independent on disk mass. Massive disks thus just give rise to more clumps that in turn increase the likelihood of clump-clump mergers, shifting the maximum stellar mass of clumps to larger values. Both approaches allow to explain the apparent scaling of the maximum clump mass with the host galaxy mass.

On the other hand, we could expect the clump properties to correlate with redshift, such that the more massive clumps should be found in the higher redshift host galaxies, since both the velocity rotation over dispersion ratio and the molecular gas fraction, which together control the Toomre disk stability criterion, have been shown to increase with redshift (Wisnioski et al. 2015; Dessauges-Zavadsky et al. 2015). However, no such a trend is observed, when plotting the measured clump stellar masses as a function of the redshift of their hosts.

If we assume that the simulations of T15 and Mandelker et al. (2017) predict correctly the stellar masses of

the order of $\sim 10^{9-9.5} M_{\odot}$ of the most massive clumps⁵, we see that still a non-negligible fraction of the observed clumps in the FS sub-sample has stellar masses above the $10^{9.5} M_{\odot}$ limit (Figures 1 and 3). Explaining these extreme clump masses with the spatial resolution effect appears difficult as several very massive clumps would need to be closely clustered. In our H α mocks (T16), maximum stellar masses up to $\sim 3 \times 10^9 M_{\odot}$ can be reached in artificially inflated ~ 1 kpc clumps. When examining these extremely massive clumps from Förster Schreiber et al. (2011) and Guo et al. (2012) individually, we find that almost all of them coincide with the centers of host galaxies or are located very close by, and have among the reddest colors. They thus appear more suggestive of galactic bulges, or alike, rather than genuine clumps (see also Elmegreen et al. 2009). But, it has also been proposed that they could be old clumps that have migrated in the centers of galaxies (Wuyts et al. 2012). Their extreme masses remain, nevertheless, puzzling. Contributions from other processes than disk fragmentation and clump-clump mergers that follow, such as minor mergers or accretion of cores of disrupted satellites (Ribeiro et al. 2016, in preparation; Mandelker et al. 2017), can be an alternative way to explain star complexes with extreme masses, eventually red colors, and central galaxy positions after migration.

4.2. Is there a characteristic clump mass from observations?

As shown in Section 3, *HST* imaging has revealed high-redshift clumps with a wide range of stellar masses, typically spread over two orders of magnitude, or significantly larger if data with different sensitivities and spatial resolutions are combined (Figure 1). Furthermore, in each clump dataset the lower stellar mass end is limited by the depth and spatial resolution of the available observations. From this we conclude that it is currently not possible to properly establish a meaningful clump stellar mass distribution from observations, and, in particular, to infer the existence and value of a characteristic clump mass. The only clear indication is that both improved sensitivity and spatial resolution shift the clump stellar mass distribution to lower masses

that ends up to be in agreement with the latest simulations of disk fragmentation. Indeed, T15 find a characteristic clump stellar mass of $\sim 5 \times 10^7 M_{\odot}$ at the onset of fragmentation and predict a stellar mass distribution of clumps, also plotted in Figure 1, which very much resembles that of clumps in the L and FD sub-samples. The agreement may well be fortuitous for the reasons just discussed.

If clumps are formed by disk fragmentation and molecular clouds down to several orders of magnitude lower mass scales are formed primarily by the same mechanism (e.g., Tasker & Tan 2009; Krumholz & Burkert 2010), clump formation would be hierarchical and, hence, one would expect clumps to continuously reveal new substructure at all scales (Elmegreen 2011; Bournaud et al. 2016), making it impossible to assess their mass distribution in a resolution-independent way. Observational evidence for a hierarchical star cluster structure in nearby galaxies is discussed by Gouliermis et al. (2015). On the other end, if high-redshift disks do possess a characteristic fragmentation mass scale as suggested by simulations of T15 and Behrendt et al. (2016), the signature of such scale should be independent on spatial resolution and sensitivity once observations approach the corresponding scale. Convergence studies of simulations with increased resolution will help assess the latter mass scale robustly in the context of the fragmentation scenario. At the same time, larger high-redshift clump samples within deep observations, ideally at the best-possible spatial resolution, and a systematic analysis (with the same clump selection criteria), including completeness corrections, are needed to establish the true clump stellar mass spectrum.

This work was supported by the Swiss National Science Foundation, in the context of the Sinergia STARFORM network on “Star formation in galaxies from the Milky Way to the distant Universe”. We are grateful to Bruce G. Elmegreen and Yicheng Guo for sharing with us their *HST* clump photometry, and we warmly thank Bruce G. Elmegreen for very fruitful discussions.

REFERENCES

Adamo, A., Östlin, G., Bastian, N., et al. 2013, ApJ, 766,

⁵ This maximum clump mass is obtained for simulated galaxies with stellar masses up to $10^{10.6} M_{\odot}$ (T15), comparable to the field galaxies in the FS sub-sample ($M_{*}^{\text{host}} \gtrsim 10^{9.8} M_{\odot}$). Limiting the simulations of T15 to galaxies with $M_{*}^{\text{host}} < 10^{10} M_{\odot}$ (comparable to galaxies in the FD and L sub-samples), leads to a clump stellar mass distribution not exceeding $\sim 10^{8.5} M_{\odot}$.

- Agertz, O., Teyssier, R., & Moore, B. 2009, *MNRAS*, 397, L64
- Bastian, N., Emsellem, E., Kissler-Patig, M., & Maraston, C. 2006, *A&A*, 445, 471
- Beckwith, S. V. W., Stiavelli, M., Koekemoer, A. M., et al. 2006, *AJ*, 132, 1729
- Behrendt, M., Burkert, A., & Schartmann, M. 2016, *ApJL*, 819, L2
- Boley, A. C., Hayfield, T., Mayer, L., & Durisen, R. H. 2010, *Icarus*, 207, 509
- Bournaud, F., Elmegreen, B. G., Teyssier, R., Block, D. L., & Puerari, I. 2010, *MNRAS*, 409, 1088
- Bournaud, F., Perret, V., Renaud, F., et al. 2014, *ApJ*, 780, 57
- Bournaud, F. 2016, *Ap&SS*, 418, 355
- Bruzual, G., & Charlot, S. 2003, *MNRAS*, 344, 1000
- Ceverino, D., Dekel, A., & Bournaud, F. 2010, *MNRAS*, 404, 2151
- Ceverino, D., Dekel, A., Mandelker, N., et al. 2012, *MNRAS*, 420, 3490
- Chabrier, G. 2003, *PASP*, 115, 763
- Dekel, A., Birnboim, Y., Engel, G., et al. 2009a, *Nature*, 457, 451
- Dekel, A., Sari, R., & Ceverino, D. 2009b, *ApJ*, 703, 785
- Dessauges-Zavadsky, M., Zamojski, M., Schaerer, D., et al. 2015, *A&A*, 577, A50
- Elmegreen, D. M., Elmegreen, B. G., Rubin, D. S., & Schaffer, M. A. 2005, *ApJ*, 631, 85
- Elmegreen, D. M., Elmegreen, B. G., & Coe, D. A. 2007, *ApJ*, 658, 763
- Elmegreen, B. G., Elmegreen, D. M., Fernandez, M. X., & Lemonias, J. J. 2009, *ApJ*, 692, 12
- Elmegreen, B. G. 2011, *ApJ*, 737, 10
- Elmegreen, B. G., Elmegreen, D. M., Sánchez, A. J., et al. 2013, *ApJ*, 774, 86
- Escala, A., & Larson, R. B. 2008, *ApJL*, 685, L31
- Fisher, D. B., Glazebrook, K., Damjanov, I., et al. 2017, *MNRAS*, 464, 491
- Förster Schreiber, N. M., Genzel, R., Bouché, N., et al. 2009, *ApJ*, 706, 1364
- Förster Schreiber, N. M., Shapley, A. E., Genzel, R., et al. 2011, *ApJ*, 739, 45
- Genel, S., Naab, T., Genzel, R., et al. 2012, *ApJ*, 745, 11
- Gouliermis, D. A., Thilker, D., Elmegreen, B. G., et al. 2015, *MNRAS*, 452, 3508
- Guo, Y., Giavalisco, M., Ferguson, H. C., Cassata, P., & Koekemoer, A. M. 2012, *ApJ*, 757, 120
- Guo, Y., Ferguson, H. C., Bell, E. F., et al. 2015, *ApJ*, 800, 39
- Kereš, D., Katz, N., Weinberg, D. H., & Davé, R. 2005, *MNRAS*, 363, 2
- Krumholz, M., & Burkert, A. 2010, *ApJ*, 724, 895
- Larsen, S. S., Efremov, Y. N., Elmegreen, B. G., et al. 2002, *ApJ*, 567, 896
- Mandelker, N., Dekel, A., Ceverino, D., et al. 2014, *MNRAS*, 443, 3675
- Mandelker, N., Dekel, A., Ceverino, D., et al. 2017, *MNRAS*, 464, 635
- Mayer, L. & Gawryszczak, A. J. 2008, in *ASPC 398, Extreme Solar Systems*, ed. D. Fischer, F. A. Rasio, S. E. Thorsett, & A. Wolszczan, 243
- Ocvirk, P., Pichon, C., & Teyssier, R. 2008, *MNRAS*, 390, 1326
- Oklopčić, A., Hopkins, P. F., Feldmann, R., et al. 2017, *MNRAS*, 465, 952
- Postman, M., Coe, D., Benítez, N., et al. 2012, *ApJS*, 199, 25
- Rodrigues, M., Hammer, F., Flores, H., Puech, M., & Athanassoula, E. 2016, *arXiv:1611.03499*, *MNRAS*, submitted
- Schaerer, D., & de Barros, S. 2010, *A&A*, 515, A73
- Sharon, K., Gladders, M. D., Rigby, J. R., et al. 2012, *ApJ*, 746, 161
- Shibuya, T., Ouchi, M., Kubo, M., & Harikane, Y. 2016, *ApJ*, 821, 72
- Tamburello, V., Mayer, L., Shen, S., & Wadsley, J. 2015, *MNRAS*, 453, 2490 (T15)
- Tamburello, V., Rahmati, A., Mayer, L., et al. 2016, *arXiv:1610.05304*, *MNRAS*, submitted (T16)
- Tasker, E. J., & Tan, J. C. 2009, *ApJ*, 700, 358
- Toomre, A. 1964, *ApJ*, 139, 1217
- Wisnioski, E., Förster Schreiber, N. M., Wuyts, S., et al. 2015, *ApJ*, 799, 209
- Wuyts, S., Förster Schreiber, N. M., Genzel, R., et al. 2012, *ApJ*, 753, 114
- Wuyts, E., Rigby, J. R., Gladders, M. D., & Sharon, K. 2014, *ApJ*, 781, 61